Photochemical & Photobiological Sciences

PAPER

Cite this: *Photochem. Photobiol. Sci.*, 2015, **14**, 1082

Enhancement of antiproliferative activity by phototautomerization of anthrylphenols†

Marijeta Kralj,*[a] Lidija Uzelac,[a] Yu-Hsuan Wang,[b] Peter Wan,[b] Martina Tireli,[c] Kata Mlinarić-Majerski,[c] Ivo Piantanida[c] and Nikola Basarić*[c]

Received 10th March 2015,
Accepted 17th March 2015

DOI: 10.1039/c5pp00099h

www.rsc.org/pps

An antiproliferative investigation was conducted on 3 human cancer cell lines, HCT 116 (colon), MCF-7 (breast), and H 460 (lung), on a series of 4 anthrylphenols in the dark and upon exposure to light (350 nm). 9-(2-Hydroxyphenyl)anthracene (**1**) moderately inhibited proliferation, but irradiation considerably enhanced the effect. The other anthracenes **4–6** exhibited antiproliferative activity in the dark, which was not enhanced upon irradiation. The enhancement of the antiproliferative effect on the irradiation of **1** was rationalized as being due to the formation of quinone methide (QM **2**) by excited state proton transfer. QM **2** acts as an electrophilic species capable of reacting with biological molecules. Although QM **2** reacts with nucleotides, the adducts could not be isolated. On the contrary, cysteine adduct **8** was isolated and characterized, whereas the adducts with glycine, serine and tripeptide glutathione were characterized by MS. Non-covalent binding of **1** to DNA and bovine serum albumin was demonstrated by UV-vis, fluorescence and CD spectroscopy. However, a straightforward conclusion regarding the DNA or protein alkylating (damaging) ability of **2** could not be drawn. The results obtained by the irradiation of **1** in the presence of DNA, amino acids and peptides, cell cycle perturbation analysis, and *in vitro* translation of GFP suggest that the effect is not only due to the damage of DNA but also due to the impact on the cellular proteins. Considering that to date all QM agents were assumed to target DNA dominantly, this is an important finding with an impact on the further development of anticancer agents based on QMs.

Introduction

Quinone methides (QMs) are ubiquitous intermediates in the chemistry of phenols.[1] The interest in the chemistry of QMs has been initiated owing to their applications in chemical synthesis[2,3] and biological activity.[4,5] It has been demonstrated that QMs react with some enzymes, such as tyrosine hydroxylases,[6] β-lactamase,[7] β-glucosidases,[8] phosphatase[9,10] or ribonuclease-A.[11] Furthermore, QMs react with nucleosides[12–15] and induce alkylation of DNA.[16–19] Some antineoplastic agents such as mitomycin,[20–22] exert their antiproliferative action on metabolic formation of QMs that alkylate DNA. Moreover, the selectivity of some naphthalene diimide-QM derivatives towards guanine-quadruplex structures has been demonstrated recently[23–25] and the reversible DNA alkylation abilities of QMs reviewed.[26]

QMs can be formed under mild conditions in the photochemical reactions[27,28] of dehydration,[29] or deamination[30,31] from the appropriately substituted phenol derivatives. Furthermore, Wan and co-workers reported that QMs can be formed from 2-phenylphenol in excited state intramolecular proton transfer reactions (ESIPT) from phenolic OH to a carbon atom of the adjacent phenyl ring.[32,33] The scope of the reaction has been extended to ESIPT in naphthylphenols,[34] BINOLs[35] and anthrylphenols.[36–38] Thus, H_2O-assisted ESIPT to the anthracene position 10 in **1** gives QM **2** that reacts with nucleophiles (H_2O, alcohols, amines) and give addition products **3** (Scheme 1).[36] Because reactions of the photogenerated QMs can be applied in the biological systems for the cross-linking of DNA,[39–43] and for the increase in the antiproliferative effect,[41,43–46] we examined whether the QMs formed by ESIPT to carbon can enhance the antiproliferative activity. Herein, we report an investigation of the antiproliferative activity on a series of anthrylphenols **1**, and **4–6** on three human cancer cell lines, HCT 116 (colon), MCF-7 (breast) and H 460 (lung) with and without exposure to irradiation, and compared to the

[a]*Department of Molecular Medicine, Ruđer Bošković Institute, Bijenička cesta 54, 10 000 Zagreb, Croatia. E-mail: Marijeta.Kralj@irb.hr; Fax: +385 1 4561 010; Tel: +385 1 4571 235*

[b]*Department of Chemistry, Box 3065, University of Victoria, Victoria, BC V8W 3V6, Canada*

[c]*Department of Organic Chemistry and Biochemistry, Ruđer Bošković Institute, Bijenička cesta 54, 10 000 Zagreb, Croatia. E-mail: nbasaric@irb.hr; Fax: +385 1 4680 195; Tel: +385 1 4561 141*

†Electronic supplementary information (ESI) available: HPLC chromatograms, NMR, MS, UV-vis, fluorescence and CD spectra. See DOI: 10.1039/c5pp00099h

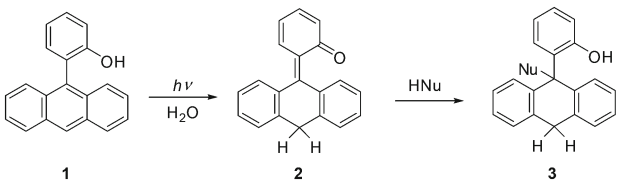

Scheme 1 Photochemical formation of QM **2** by H_2O-assisted ESIPT and reaction with nucleophiles.

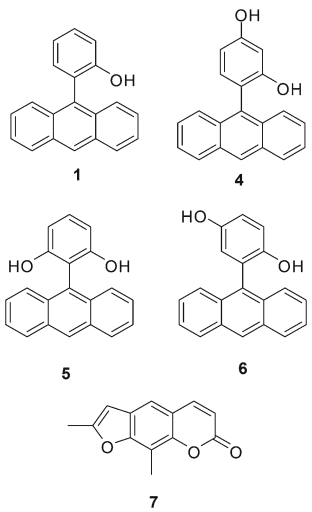

Fig. 1 Structures of anthrylphenols **1**, **4–6** undergoing H_2O-assisted ESIPT and psoralen derivative **7**.

activity of psoralen **7** (Fig. 1). Enhancement of the antiproliferative effect was observed for **1**, so additional experiments were performed to elucidate the mechanism of the antiproliferative action including an assessment of non-covalent binding to DNA and proteins, alkaline DNA electrophoresis, inhibition of green fluorescence protein (GFP) translation *in vitro* and influence on cell cycle of tumor cells. The results showed that DNA is not the only target of QMs leading to antiproliferative activity, as has been postulated in most of the reports. Proteins[47] and enzymes[6–11] are also viable QM targets.

Experimental

General

Compounds **1** and **4–6** were prepared according to the previously described procedure.[36–38] The chemicals for synthesis were purchased from the usual suppliers, whereas the solvents for the synthesis and chromatographic separations were purified by distillation, or used as received (p.a. grade). Prior to the spectroscopic investigations, **1** was also purified by crystallization from dichloromethane/cyclohexane. The ^1H and ^{13}C NMR spectra were recorded on a Bruker AV-300, 500 or 600 MHz. The NMR spectra were taken in $CDCl_3$ or DMSO-d_6 at rt using TMS as a reference. For sample analysis, a Shimadzu HPLC equipped with a Diode-Array detector and a Phenomenex Luna 3u C18(2) column was used. The mobile phase was CH_3OH–H_2O (20%). Alternatively, an HPLC Agilent 1200 Series and triple quadrupole mass spectrometer Agilent 6410 was used. MS was also obtained on an Amazon ETD, Bruker Daltonik (ESI-MS or MALDI-TOF). For the chromatographic separations, silica gel (Merck 0.05–0.2 mm) or aluminum oxide (activity IV/V) were used. Analytical thin layer chromatography was performed on Polygram® SILG/UV_{254} (Machery-Nagel) plates. In the irradiation experiments, CH_3CN was of HPLC purity and mQ-H_2O (Millipore) was used. ct-DNA and BSA were purchased from Aldrich.

Analytical irradiation experiments in the presence of DNA bases

Anthracene **1** (15 mg, 0.055 mmol) was dissolved in CH_3CN (60 mL) and divided into four cuvettes (4 × 15 mL) to which aqueous solutions of sodium phosphate buffer (4 × 2 mL, pH = 6.8, 0.1 M) were added. To the first cuvette, adenine (2 mg, 0.015 mmol) was added, to the second cytosine (2 mg, 0.018 mmol) and to the third guanine (2 mg, 0.013 mmol). The solutions were purged with Ar for 30 min, sealed with a septum and simultaneously irradiated in a Luzchem reactor equipped with 8 lamps with the output at 350 nm over 1 h. The composition of the irradiated solutions was analyzed by HPLC (see the ESI†).

Preparative irradiation in the presence of cytosine

Anthracene **1** (20 mg, 0.074 mmol) was dissolved in CH_3CN (30 mL) and mixed with an aqueous solution of sodium phosphate buffer (20 mL, pH = 6.8, 0.1 M) and cytosine (20 mg, 0.18 mmol) suspended in CH_3CN (100 mL). The resulting mixture was purged with Ar for 30 min and irradiated in a Rayonet reactor equipped with 11 lamps with the output at 350 nm during 1 h. The course of the reaction was followed by HPLC. During the irradiation, the solution was purged continuously with Ar and cooled with a tap-H_2O finger-condenser. After the irradiation, H_2O (50 mL) was added and extraction with CH_2Cl_2 (2 × 75 mL) and EtOAc (2 × 75 mL) was carried out. The organic extracts were combined and dried over anhydrous $MgSO_4$. After filtration, the solvent was removed on a rotary evaporator and the residue was chromatographed on a thin layer of silica using CH_2Cl_2/EtOAc (10%) as eluent. In addition to **1** that is recovered, a fraction (5 mg) was isolated that contained a mixture of compounds with possible cytosine adducts (see the ESI†).

Irradiation in the presence of glycine ethyl ester

Anthracene **1** (100 mg, 0.37 mmol) was dissolved in CH_3CN (150 mL) and mixed with a solution of glycine ethyl ester (2.0 g, 14 mmol) in aqueous phosphate buffer (50 mL, pH = 7, c = 0.05 M), or H_2O (50 mL) to which pH was adjusted to 9.5 with NaOH prior to the mixing with the solution of **1**. The resulting CH_3CN–H_2O solutions were purged with Ar for 30 min and irradiated in a Rayonet reactor equipped with

11 lamps with the output at 350 nm during 2 h. After irradiation, the solution was analyzed by ESI-MS. H_2O (100 mL) was added and the extraction with CH_2Cl_2 (3 × 75 mL) was carried out. The organic extracts were dried over anhydrous $MgSO_4$, filtered and the solvent was removed on a rotary evaporator. The residue was chromatographed on a silica gel or alumina column using CH_2Cl_2/EtOAc (0–100%) as the eluent. Chromatographic separation furnished the starting compound **1** (40–50 mg), and a mixture of unidentified rearrangement products.

Irradiation in the presence of serine or glutathione

Anthracene **1** (15 mg, 0.055 mmol) was dissolved in CH_3CN (10 mL) and mixed with a solution of (±) serine (120 mg, 1.14 mmol) or L-glutathione (150 mg, 0.49 mmol) in H_2O (10 mL). The solutions were poured into cuvettes, sealed with a septum, purged with Ar for 30 min, and irradiated in a Luzchem reactor equipped with 8 lamps with the output at 350 nm over 1 h. After irradiation, the composition of the solutions was analyzed by ESI-MS.

Preparative irradiation in the presence of protected cysteine

Anthracene **1** (70 mg, 0.26 mmol) was dissolved in CH_3CN (70 mL) and mixed with a solution of methy ester of *N*-acetyl-L-cysteine (350 mg, 2 mmol in 80 mL CH_3CN) and H_2O (30 mL). The resulting solution was purged with Ar for 30 min and irradiated in a Rayonet reactor equipped with 11 lamps with the output at 350 nm during 2 h. During irradiation, the solution was purged continuously with Ar and cooled with a tap-H_2O finger-condenser. After the irradiation the solvent was removed on a rotary evaporator and the residue chromatographed on a column of silica using CH_2Cl_2/EtOAc (10%) as the eluent, and rechromatographed on a TLC using the same eluent. Chromatography furnished 20 mg (28%) of the starting material, 40 mg (34%) of the cysteine adduct and 10 mg of a mixture containing H_2O-adduct **3** along with some unidentified products.

(*R*)-Methyl 2-acetamido-3-[9-(2-hydroxyphenyl)-9,10-dihydroanthracen-9-ylthio]propanoate (8). 40 mg (34%); yellowish oil, ^{1}H NMR (300 MHz, $CDCl_3$) δ/ppm 8.05 (dd, 1H, J = 1.5 Hz, J = 7.8 Hz), 7.34–7.42 (m, 3H), 7.26–7.34 (m, 2H), 7.08–7.18 (m, 3H), 6.78–7.85 (m, 3H), 5.62 (d, 1H, J = 7.7 Hz), 4.28–4.44 (m, 3H), 4.14 (br s, 1H), 3.60 (s, 3H, OCH_3), 2.79 (dd, 1H, J = 4.5 Hz, J = 13.0 Hz), 2.66 (dd, 1H, J = 6.1 Hz, J = 13.0 Hz), 1.85 (s, 3H, $COCH_3$); ^{13}C NMR (75 MHz, $CDCl_3$) δ/ppm 170.7 (s), 169.4 (s), 153.5 (s), 137.2 (s), 137.1 (s), 136.0 (s), 135.9 (s), 131.2 (d), 129.8 (d), 128.2 (d), 128.1 (d, 2C), 128.0 (d), 127.6 (s), 127.2 (s), 127.1 (s), 126.7 (d), 126.6 (d), 120.4 (d), 117.9 (d), 65.4 (s), 52.4 (d), 51.1 (q), 35.4 (t), 34.0 (t), 22.9 (q), 14.1 (q); ESI-MS (m/z) 470 (M^+ + Na); HRMS (MALDI) calculated for $C_{20}H_{15}O$ 271.1117, found 271.1118; calculated for $C_6H_{10}NO_3S$ 176.0376 found 176.0330.

Spectroscopic measurements

Stock solutions of anthracene **1** in DMSO (c = 0.01 M), ct-DNA (c = 0.01 M) in aqueous sodium cacodylate buffer (pH = 7, c = 0.05 M), and bovine serum albumin (BSA, c = 0.15 mM) in potassium phosphate buffer (pH = 7, c = 1 mM) were prepared. The solutions were diluted further with the cacodylate or the phosphate buffer, respectively. The UV-VIS spectra were recorded on a Varian Cary 100 Bio spectrophotometer at rt. The fluorescence spectra were obtained on a Varian Cary Eclipse fluorometer and the concentrations were adjusted to absorbances of less than 0.1 at excitation wavelengths of 270, 280, 290, 295, 346 or 365 nm. The solutions were not purged.

In the study of the interaction with DNA, the UV-vis spectra of **1** (1×10^{-5} M) in the cacodylate buffer were recorded in the presence of ct-DNA (1×10^{-4} M) at different temperatures (25–95 °C). Thermal melting curves for DNA and the complexes with studied compounds (c(DNA) = 2×10^{-5} M; compound/DNA ratio r = 0.2) were determined as previously described[48] by following the absorption change at 270 nm as a function of temperature. The T_m values are the inflection points of the transition curves determined from the maximum of the first derivative, and were checked graphically using the tangent method. The ΔT_m corresponds to the difference in the T_m of the free nucleic acid T_m of the complex. The CD spectra were recorded on a Jasco J-815 spectrometer in the cacodylate buffer with ct-DNA (c = 4×10^{-5} M) and **1** (c = 1×10^{-5} M) in 3 mL cuvettes at rt.

In the study of the interaction with bovine serum albumin (BSA), the UV-vis, fluorescence and CD spectra of **1** (1×10^{-5} M) in the phosphate buffer were recorded in the presence of BSA (3×10^{-6} M) in 3 mL cuvettes at 25 °C.

Antiproliferative investigation

The experiments were carried out on three human carcinoma cell lines HCT 116 (colon), MCF-7 (breast) and H 460 (lung). The cells were cultured as monolayers and maintained in Dulbecco's modified Eagle medium (DMEM) supplemented with 10% fetal bovine serum (FBS), 2 mM L-glutamine, 100 U mL^{-1} penicillin, and 100 μg mL^{-1} streptomycin in a humidified atmosphere containing 5% CO_2 at 37 °C.

The cells were inoculated in parallel on three 96-well microtiter plates on day 0, at 1×10^4 (HCT 116 and H 460) or 3×10^4 cells ml^{-1} (MCF-7), depending on the doubling times of a specific cell line. The test agents were added in ten-fold dilutions (10^{-8} to 10^{-4} M) the next day and incubated for a further 72 h. Working dilutions were freshly prepared on the day of testing. One of the plates was left in the dark, the other one was irradiated in a reactor (6 lamps 350 nm, 1 min) 4, 24 and 48 hours after adding the compounds (3 × 1 min), while the third one was irradiated in a reactor (6 lamps 350 nm, 5 min) 4, 24, and 48 hours after the addition of the compounds (3 × 5 min). After 72 h of incubation, the cell growth rate was evaluated by performing the modified MTT assay[44–46] (for the irradiated and non-irradiated cells), which detects dehydrogenase activity in viable cells. The absorbance (A) was measured on a microplate reader at 570 nm. The absorbance was directly proportional to the number of living, metabolically active cells. The percentage of growth (PG) of the cell

lines was calculated using one or the other of the following two expressions:

$$\text{If } (\text{mean } A_{\text{test}} - \text{mean } A_{\text{tzero}}) \geq 0, \text{then PG} = 100 \times (\text{mean } A_{\text{test}} - \text{mean } A_{\text{tzero}})/(\text{mean } A_{\text{ctrl}} - \text{mean } A_{\text{tzero}}).$$

$$\text{If } (\text{mean } A_{\text{test}} - \text{mean } A_{\text{tzero}}) < 0, \text{then PG} = 100 \times (\text{mean } A_{\text{test}} - \text{mean } A_{\text{tzero}})/A_{\text{tzero}},$$

where the mean A_{tzero} is the average of the absorbance measurements before exposing cells to the test compound, the mean A_{test} is the average of absorbance measurements after the desired period of time, and the mean A_{ctrl} is the average of absorbance measurements after the desired period of time with no exposure of the cells to the test compound. In the experiments where the cells were irradiated, A_{ctrl} represents the irradiated control cells. After irradiation at 350 nm (3 × 5 min) up to 25% growth inhibition compared to A_{ctrl} without irradiation was observed. The results are expressed as IC_{50}, which is the concentration necessary for 50% inhibition. The IC_{50} values were calculated from the concentration-response curves using linear regression analysis by fitting the test concentrations that give PG values above and below the reference value (*i.e.* 50%). Each test was performed in quadruplicate in at least two individual experiments.

Cell cycle analysis

Colon cancer cells, HCT 116, were seeded into 6-well plates (2×10^5 per well). After 24 hours, the tested compounds were added at various concentrations (as shown in the Results section). One of the plates was left in the dark, while the other was irradiated in a reactor (6 lamps 350 nm, 5 min) 4, 24 and 72 hours after the addition of the compounds. After the desired length of time (48 or 72 hours), the attached cells were trypsinized, combined with floating cells, washed with phosphate buffer saline (PBS), fixed with 70% ethanol, and stored at −20 °C. Immediately before analysis, the cells were washed with PBS and stained with 50 μg ml^{-1} of propidium iodide (PI) with the addition of 0.2 μg μl^{-1} of RNAse A. The stained cells were then analyzed by Becton Dickinson FACScalibur (Becton Dickenson) flow cytometry (20 000 counts were measured). The percentage of cells in each cell cycle phase was determined using ModFit LT™ software (Verity Software House) based on the DNA histograms. The tests were performed in duplicate and repeated at least twice.

Alkaline agarose gel assay

DMSO-stock solutions of compounds **1** and **7** (psoralen) were diluted in H_2O and used for the reactions. Plasmid pCI (0.8 μg per sample) was mixed with compound dilutions. The reaction mixtures were irradiated for 5 min at 350 nm in a Luzchem reactor. The irradiated solutions were added to alkaline agarose gel loading buffer [50 mM NaOH, 1 mM ethylenediaminetetraacetic acid (EDTA), 3% Ficoll, and 0.02% bromophenol blue] and loaded on a 1% alkaline agarose gel containing 50 mM NaOH and 1 mM EDTA. The gels were run in 50 mM NaOH and 1 mM EDTA at a 25 V constant voltage in a horizontal electrophoresis system (BIO-RAD, USA), stained with ethidium bromide (0.5 μg mL^{-1}) for 10 min, after neutralization of the gel with 30 mM Tris-HCl (pH 7.5). The resulting products were visualized and documented with UV light at 254 nm (Uvitec, Cambridge).

Inhibition of *in vitro* translation

Compound **1** was tested for its inhibitory effect on the translation of Enhanced Green Fluorescence Protein (EGFP) using an *E. coli* derived cell-free protein synthesis system (S30 T7 High-Yield Protein Expression System, Promega, USA) according to the manufacturer's protocol, as described previously.[49] This system can produce high levels of recombinant proteins if supplemented with an appropriate expression plasmid, T7 RNA polymerase for transcription, and other necessary components for translation, such as amino acids. Briefly, 500 ng of pEGFP–C1 plasmid (Clontech, USA) was incubated with water or the tested compound (at 100 μM concentration) and was irradiated at 350 nm for 5 min, or kept in dark at 24 °C. Along with the tested compounds psoralen, a known intercalative agent, which, upon exposure to ultraviolet (UVA) radiation, can form covalent interstrand cross-links (ICL) (5 μM concentration, Sigma) was also used for comparison purposes. Positive controls containing the plasmid in sterile water and negative controls did not contain DNA template (plasmid), respectively. Subsequently, the protein expression system was deployed according to the manufacturer's recommendations and protocol with slight modification of incubation temperature to ensure the optimal EGFP folding. Instead of 37 °C the mixture was incubated at 32 °C for 3 hours. Afterwards, the GFP fluorescence was recorded on microtiter plates using Fluoroskan Ascent Microplate Fluorometer (excitation at 485 nm, emission at 538 nm; ThermoScientific). The mean fluorescence of the negative controls was subtracted from the means of the tested and control samples, and the percentages from the control were calculated. A minimum three experiments were performed, and the statistical difference was calculated using the Microsoft Excel *t*-test.

Results and discussion

Chemistry

Synthesis of compounds **1** and **4–6** and their photochemical reactivity have been described.[36–38] They were obtained by Suzuki coupling reactions, followed by a cleavage of the methyl ethers by BBr_3.[36–38]

Irradiation of **1** in CH_3CN–H_2O gives H_2O-adduct **3** (Nu = OH) that can be isolated by chromatography.[36] In addition, we investigated the reactivity of photogenerated QM **2** with nucleobases. Irradiations of **1** in CH_3CN–H_2O were performed in the presence of adenine (A), guanine (G) and cytosine (C). In a typical photochemical experiment, a mixture of **1** (0.1 mmol) and a nucleobase (≈0.1 mmol), were dissolved in a mixture of CH_3CN–H_2O containing phosphate buffer

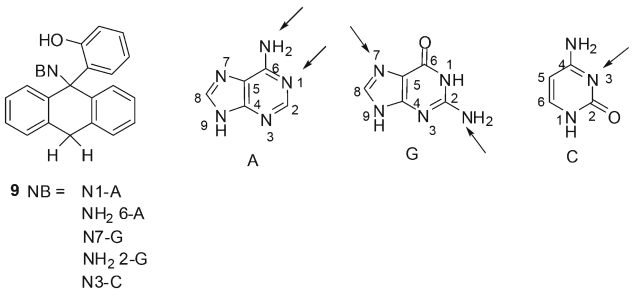

Fig. 2 Tentative structures **9**, adducts of the nucleobases to QM **2**.

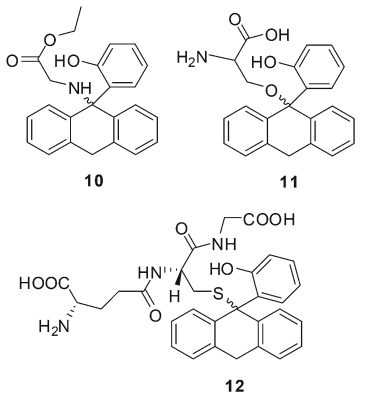

Fig. 3 Tentative structures of **10**, **11** and **12**, adducts of the amino acids and glutathione to QM **2**.

(c = 0.1 M, pH = 6.8) and irradiated 1 h at 350 nm. The course of the reaction was followed by HPLC. The irradiations gave H_2O-adduct **3** and additional products that were not detected when irradiation was performed without the nucleobases. Therefore, the structures were tentatively assigned to adducts of the nucleobases to QM **2** (Fig. 2). However, no adduct was isolated. The photoproducts decomposed after standing in a CH_3CN–H_2O solution at rt for several hours. Upon attempts to purify the photoproducts by preparative TLC on silica, they decomposed to **1** and nucleobase, and gave some additional complex rearrangement products that were not analyzed. Therefore, the site of the attack to the nucleobases could not be determined. The drawings in Fig. 2 correspond to the anticipated sites of attack according to the published reactivity of the QMs with deoxynucleosides.[12–15]

The reactivity of the photogenerated QM **2** was also investigated with amino acids. The irradiation of **1** in CH_3CN–H_2O was performed in the presence of C-protected glycine, serine and N- and C-protected cysteine. Irradiation in the presence of glycine ethyl ester was performed at pH 7 and pH 9.5. In a neutral solution, no glycine adducts were detected. Chromatographic separation on silica recovered the starting anthracene (40%) and gave H_2O-adduct **3** in addition to a mixture of unidentified products (40%). On the contrary, after irradiation of the solution at pH 9.5, corresponding to the pK_a of glycine, adduct **10** (Fig. 3) could be detected by NMR and ESI-MS-MS (see the ESI†). However, attempts to isolate **10** on silica gel or alumina gave starting compound **1** (50%) and a mixture of H_2O-adduct and some rearranged products (30%). The experiments indicate that amino groups in amino acids or peptides can in principle react with QM **2**. However, the addition is feasible only at high pH when the amino groups are not protonated.

Methanol is a good nucleophile that can react with QM **2** giving adducts.[36] Consequently, it is plausible that QM **2** can react with other alcohols or amino acids and peptides bearing free OH group such as serine. Indeed, the irradiation of **1** in CH_3CN–H_2O in the presence of nonprotected serine in neutral solution gave an adduct that was detected by ESI-MS (se the ESI†). MS-MS analysis of the isolated molecular ion (m/z 376) gave major peaks of m/z 271 and 106, corresponding to the protonated **1** and serine, respectively, in accordance with the high aptitude of molecule to decompose to the starting materials. We could not isolate the product, but its structure probably corresponds to ether **11**. At pH 7 the hydroxyl group in serine is a much better nucleophile than the protonated amino group.

Irradiation of **1** in CH_3CN–H_2O in the presence of N- and C-protected cysteine, followed by chromatographic separation gave cysteine adduct **8** (34%, Scheme 2), together with the recovered starting material (28%), and some unidentified products. Although adduct **8** can be present in two diastereomeric forms, only one isomer was isolated. The structure assignment of **8** was straightforward from the ^{1}H and ^{13}C NMR spectra. However, stereochemistry at the stereogenic center formed in the photochemical reaction could not be assigned. In the aliphatic part of the ^{1}H NMR spectrum, a characteristic signal corresponding to the dihydroanthracene H-atoms were observed in a multiplet at δ 4.2–4.4 ppm, together with the signal of H-atom at the cysteine chiral center. In the aromatic part of the ^{13}C NMR spectrum, twelve doublets were detected together with the singlets of two carbonyls and four aromatic C-atoms. The aliphatic part of the ^{13}C NMR spectrum revealed two triplets, one doublet and two quartets, all in accordance with the assigned structure.

To demonstrate the ability of QM to react with oligopeptides, the irradiation of **1** in CH_3CN–H_2O in the presence of glutathione was conducted. After irradiation, the solution was analyzed by ESI-MS (see the ESI†), which detected the presence of an adduct whose structure was tentatively assigned to **12**. MS-MS analysis of the isolated molecular ion (m/z 578) gave

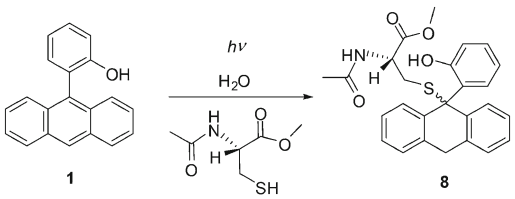

Scheme 2 Photochemical formation of cysteine adduct **8**.

major peaks of *m*/*z* 271, 308, and 449 corresponding to the protonated **1**, glutathione and a fragment after the loss of 2-amino-5-oxopentanoic acid, respectively. The fragmentation of the molecule clearly indicated that glutathione sulfur is attached to the dihydroanthracene moiety, which is in accordance with structure **12**.

Photocytotoxicity study

The antiproliferative effect of the photogenerated QMs on three cancer cell lines, HCT 116 (colon carcinoma), MCF-7 (breast carcinoma), and H 460 (lung carcinoma), was investigated with 4 anthracene derivatives. Psoralen derivative **7** was used as a positive reference compound that is known to exhibit antiproliferative activity on photoactivation.[43] The cells were incubated with the compounds and kept in the dark, or irradiated at 350 nm 3 × 1 min or 3 × 5 min. The activities expressed as IC_{50} (concentration that causes 50% inhibition of the cell growth) are compiled in Table 1. Without irradiation, all compounds exerted mild antiproliferative activity in the micromolar concentration range, without a specific effect with respect to the cell type. Irradiation induced enhancement of the activity for derivatives **1** and **6**, and the effect could clearly be correlated to the irradiation time, probably due to the formation of the corresponding QMs. Up to a 10-fold and 3-fold increase in activity was achieved for **1** and **6**, respectively. Although the enhancement for psoralen derivative **7** is more pronounced (more than 100-fold), **1** was chosen as a candidate compound for further studies for the elucidation of the antiproliferation mechanism.

Non-covalent binding to DNA

Anthracene derivatives are generally good candidates for the non-covalent binding to DNA, either by intercalation or binding to a minor groove. Non-covalent binding of **1** to calf thymus DNA (ct DNA) was investigated by UV-vis and CD spectroscopy. The absorption spectrum of **1** ($c = 1 \times 10^{-5}$ M) in an aqueous solution in the presence of cacodylate buffer (50 mM, pH = 7) exhibits typical structured anthracene absorption at 320–400 nm. Heating of the solution to 70 °C and cooling to the rt induces the disappearance of an anthracene absorption band with a concomitant increase in the spectral baseline, suggesting aggregation of the molecules and the formation of nanoparticles that cause light scattering. The addition of an aqueous solution of ct DNA to a solution of **1** resulted in a hypochromic change in the absorption band at 320–400 nm, suggesting the binding of **1** to the DNA. However, an increase in temperature to 70 °C induced an increase in absorbance, suggesting dissociation of the complex of DNA and **1** (Fig. 4).

Compounds that bind to DNA cause stabilization of the duplex and increase the DNA melting temperature (ΔT_m)[48]. Although the absorption spectra (Fig. 4) indicated DNA/**1** complex formation, **1** did not stabilize ds-DNA against thermal denaturation. A possible explanation is related to the observed aggregation of **1**. Nevertheless, the irradiation of DNA in the presence of **1** at rt is anticipated to cause the alkylation of DNA, resulting DNA adducts that show higher thermal stability than non-treated DNA. However, determination of T_m for DNA in the absence of **1**, and in the presence of **1** after 5 min of irradiation at 350 nm, gave the same $T_m = 79.0 \pm 0.3$ °C. This lack of measurable stabilization could be due to the low efficiency of adduct formation or because of the instability of nucleobase-adducts **9** (Fig. 2). Therefore, the thermal denaturation experiment could not give an unambiguous conclusion with respect to the ability of QM **2** to alkylate DNA.

CD spectroscopy as a highly sensitive method to assess the conformational changes in the secondary structure of poly-

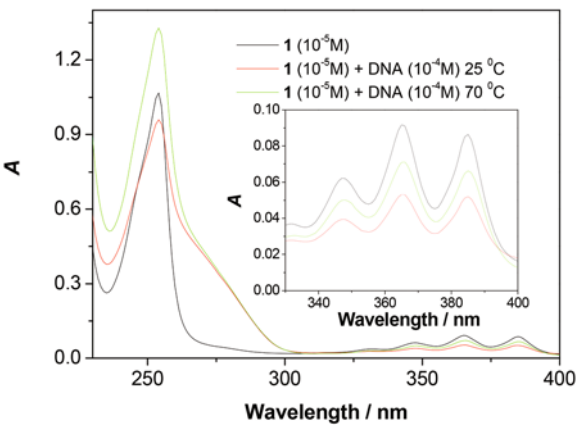

Fig. 4 Absorption spectrum of **1** ($c = 1 \times 10^{-5}$ M) in aqueous cacodylate buffer (50 mM, pH = 7) in the presence of ct-DNA ($c = 1 \times 10^{-4}$ M) at different temperatures; inset: enlarged part of the spectra between 330 and 400 nm.

Table 1 IC_{50} values (in μM)[a] induced with compounds **1** and **4–7** with and without irradiation at 350 nm

	HCT116			MCF-7			H 460		
Comp.	Not irrad.	3 × 1 min	3 × 5 min	Not irrad.	3 × 1 min	3 × 5 min	Not irrad.	3 × 1 min	3 × 5 min
1	21 ± 4	12 ± 2	2 ± 0.2	20 ± 4	8 ± 5	2 ± 0.3	20 ± 4	13 ± 1	2 ± 0.2
4	24 ± 2	23 ± 4	19 ± 1	24 ± 2	22 ± 1	17 ± 2	18 ± 1	19 ± 1	15 ± 2
5	18 ± 1	18 ± 2	10 ± 2	17 ± 2	14 ± 3	6 ± 2	18 ± 0.4	18 ± 2	12 ± 1
6	21 ± 1	19 ± 0.1	11 ± 0.02	17 ± 3	15 ± 3	5 ± 0.2	17 ± 3	16 ± 1	9 ± 3
7	39 ± 24	0.1 ± 0.1	<0.01	3 ± 1	0.2 ± 0.1	0.02	≥100	0.03 ± 0.01	<0.01

[a] Concentration that causes 50% inhibition of tumor cell growth.

nucleotides was applied to investigate the mode of binding of **1** to ct-DNA. It was anticipated that binding of achiral **1** to the helically chiral DNA should give rise to the induced CD spectrum of **1**, in addition to the expected changes in the CD spectrum of DNA (220–300 nm).[50] However, no change was observed between the CD spectrum of free ct DNA, and DNA ($c = 4 \times 10^{-5}$ M) in the presence of **1** ($c = 1 \times 10^{-5}$ M). This indicates that **1** does not form a dominant complex within well defined DNA binding site (*e.g.* intercalation or minor groove binding), but rather aggregates nonspecifically along both grooves of the polynucleotide double helix due to the hydrophobic effect and aromatic interactions between molecules of **1** (latter supported by hypochromic changes in the UV-vis spectra, Fig. 4). Nevertheless, even such nonspecific aggregation brings **1** close to the number of potential alkylation sites along DNA. Therefore, to check if the photochemical reaction could lead to the changes in the CD spectra due to alkylation with QM **2**, the solution **1** in the presence of ct-DNA was irradiated (5 min, 8 lamps at 350 nm). However, no change in the CD spectrum could be observed, either due to a lack of measurable reactivity of QM **2** with DNA, or because the photochemical product does not induce significant changes in the DNA helical chirality.

Non-covalent binding to proteins and photoreaction in protein

Anthracene derivative **1** is nonpolar, so it is plausible that it could bind to the hydrophobic pockets of the proteins. It has been demonstrated that anthracenes bind to bovine serum albumin (BSA) undergo photochemical reactions.[51] Therefore, non-covalent binding of **1** to BSA was investigated by UV-vis, fluorescence and CD spectroscopy. After the addition of an aqueous BSA solution to the solution of **1** ($c = 1 \times 10^{-5}$ M) in phosphate buffer (pH = 7, $c = 1$ mM), a hyperchromic change in the absorption bands at 250 and 320–400 nm was observed (Fig. 5 top). The hyperchromic change suggests that **1** binds to BSA upon which it deaggregates. After the addition of BSA ($c = 3 \times 10^{-6}$ M) to the solution of **1** ($c = 1 \times 10^{-5}$ M) in phosphate buffer (pH = 7, $c = 1$ mM), a positive signal in the CD spectrum was observed at 250–260 nm, corresponding to the $S_0 \rightarrow S_2$ anthracene absorption (Fig. 5. bottom). In the region, 350–400 nm, the CD signal was not observed due to the much lower absorptivity. The induced CD spectrum strongly indicates the non-covalent binding of achiral **1** to the protein. Similar induced CD spectra of anthracene derivatives in BSA with a positive signal at 250–260 nm have been reported.[51]

The fluorescence excitation and emission spectra of **1** ($c = 1 \times 10^{-5}$ M) in aqueous phosphate or cacodylate buffer indicate the aggregation of molecules (see the ESI†). In contrast to the vibronically well resolved emission spectrum of **1** in CH_3CN,[36] in aqueous buffered solution, the spectrum (regardless of the excitation wavelength, 270, 280, 345 or 365 nm) has a shoulder at 395 nm, most probably corresponding to the non-aggregated molecules, and much stronger band with a maximum at 430 nm, corresponding to the emission from the aggregated molecules (Fig. 5 middle and ESI†). In a fluorescence spectrum of **1** and BSA mixture, fluorescence from both species can be detected. However, the fluorescence from the protein was quenched compared to that of the neat BSA solution of the same concentration, whereas the anthracene emission was stronger and more resolved. This observation can be explained by non-covalent binding of **1** to BSA, whereupon the anthracene molecules deaggregate. Moreover, the formation of the BSA/**1** complex leads to the quenching of fluorescence from tryptophanes in the protein by energy transfer to **1**. Consequently, fluorescence from **1** is stronger in the complex than in the aqueous solution not containing BSA.

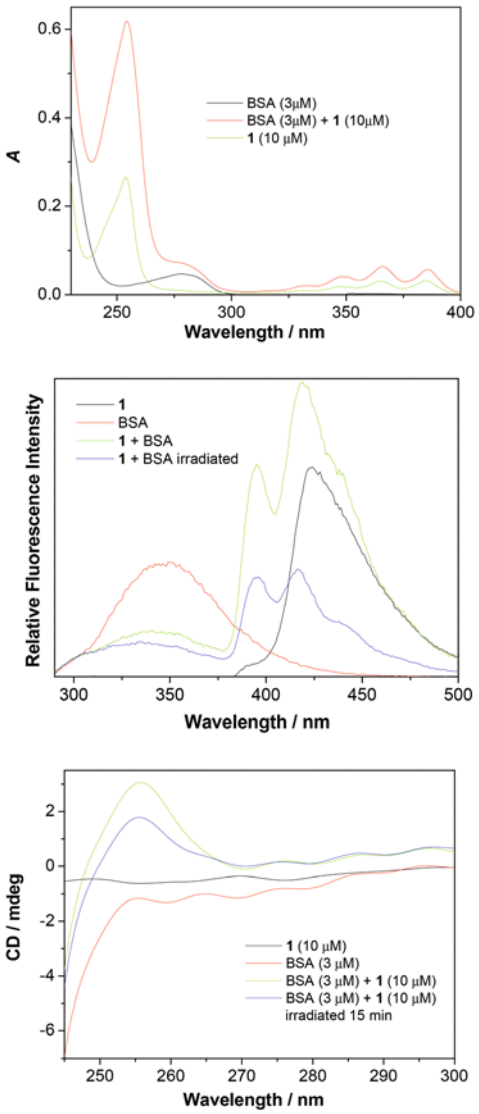

Fig. 5 Absorption (top), fluorescence (middle, λ_{ex} = 280 nm), and CD spectra (bottom) of **1** ($c = 1 \times 10^{-5}$ M), BSA ($c = 3 \times 10^{-6}$ M) and their mixture in aqueous phosphate buffer (1 mM, pH = 7) at 25 °C before and after irradiation (Luzchem, 8 × 350 nm, 15 min).

The irradiation of **1** (Luzchem, 350 nm, 15 min) in the presence of BSA resulted in the bleaching of the typical anthracene absorption band (see the ESI†) and the decrease of fluorescence, in agreement with the photoreaction of **1** giving

anthracene adducts. Furthermore, the induced CD spectrum in the region 250–260 nm was weaker after the irradiation, indicating that anthracene bound in the protein underwent photoreaction. The photoreaction inside the protein could be due to the photoreaction with BSA or due to photohydration giving H_2O-adduct **3**. An attempt to detect the MS of the BSA-anthracene photo-adducts by MALDI failed. However, no unambiguous conclusion could be made due to too high molecular weight of BSA and a small *m*/*z* difference between the potential adduct and the BSA M^+ for which MALDI analysis is not sensitive enough.

DNA alkylation experiment

To check the DNA-alkylation ability, we performed the irradiations of supercoiled plasmid DNA in the presence of compound **1** and **7** (psoralen), followed by alkaline DNA gel electrophoresis. Clear differences in the various plasmid forms' migration performance could be seen after the irradiation of plasmid DNA in the presence of **7**, due to its well-known ability to intercalate and, upon exposure to ultraviolet radiation, form covalent interstrand cross-links (ICL) (Fig. 6).

Interstrand cross-linking (XL) activities of psoralen were evident as X-bands of circular (X-C), open circular (X-OC) and linear X-L forms). However, no X-bands and no difference in migratory ability compared to control DNA were observed after irradiation of **1**. Such results are not surprising because the DNA alkylation products of **1** decompose very easily, and alkaline agarose gel electrophoresis can distinguish between cross-linked and uncross-linked species, but is probably not sensitive enough to visualize mono-alkylation,[52] which we expected to occur after the irradiation of **1**.

Cell cycle perturbation

To shed more light on the antiproliferative mechanism(s) of **1**, we assessed its influence on the cell cycle of HCT 116 cells at the IC_{50} concentration obtained for both non-irradiated (20 μM; data not shown), irradiated (2 μM), along with a 0.2 μM concentration after 48 h and 72 h of incubation with or without 2 × 5 min, or 3 × 5 min of irradiation, respectively. Interestingly, without irradiation, compound **1** negligibly influences the cell cycle, mostly causing a slight delay in the S phase-progression (DNA synthesis), and a slight induction of subG1 cells (Fig. 7b). These results do not point to the DNA intercalative mode of action (usually strong G2/M arrest) and are in accordance with the previously described study of non-covalent DNA binding. The irradiation of cells for 2 × 5 min incubated with a 2 μM concentration of **1**, caused a strong decrease in the number of cells in the S phase, induced both G1 and G2/M phase arrest and significantly increased the number of cells in subG1, pointing to the activation of apoptosis (Fig. 7a). The additional 5 min of irradiation (72 h of incubation) led to the massive activation of apoptosis (Fig. 7b). While these results clearly demonstrate a strong influence on the cell cycle and induction of cell death, the qualitative outcomes do not undoubtedly point to DNA damage caused by DNA alkylation as a trigger. Specifically, it has been previously demonstrated in the same tumor cell model (HCT 116 cells) that different alkylating agents, which induce either mono-

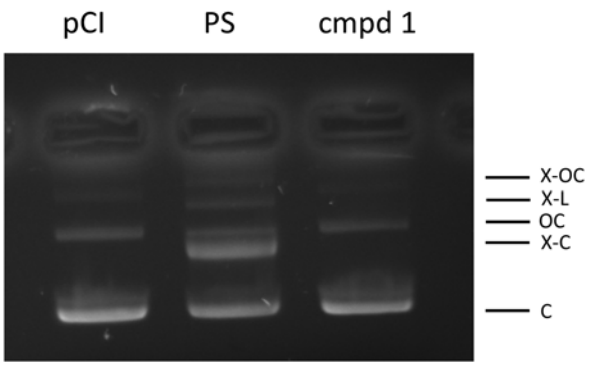

Fig. 6 Alkaline gel electrophoresis of DNA in the presence of psoralen and **1** (lane 1: irradiated pCI 0.8 μg, lane 2: irradiated pCI + psoralen (PS), 5 μM, lane 3: irradiated pCI + **1** 100 μM) after irradiation (5 min at 350 nm). Non-reacted circular and open-circular plasmid forms (C and OC) and their cross-linked species (X-C and X-OC) along with cross-linked linear (X-L) are indicated at the right side of the gel image.

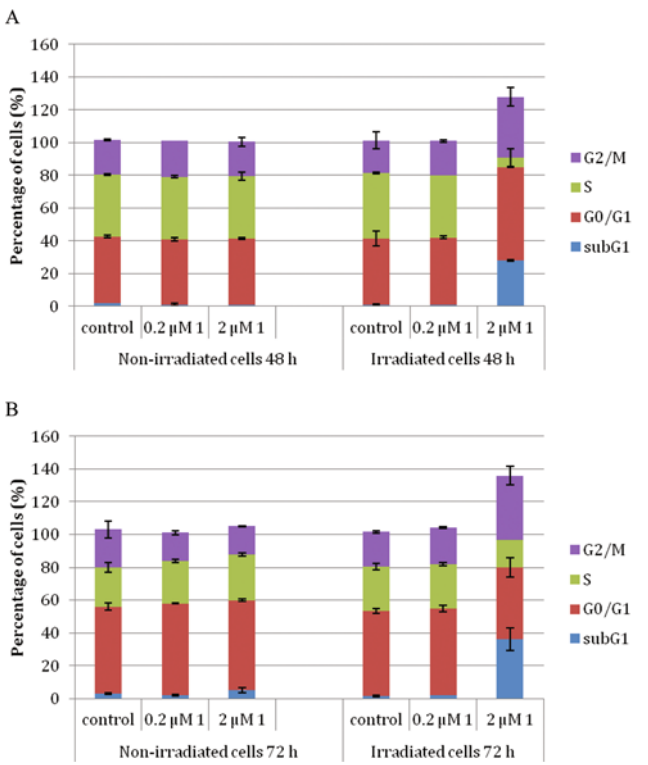

Fig. 7 The effects of compound **1** at 0.2 and 2 μM concentrations on the cell cycle distribution of HCT 116 cells after 24 and 48 h treatments (see text for details). The histograms represent the percentage of cells ± sd in the respective cell cycle phase (G1, S and G2/M), along with the percentage of cells in the subG1 (dead/apoptotic cells) obtained by flow cytometry.

alkylation of DNA or DNA cross-links, induced strong G2/M arrest.[53] Similar observations have also been made in other tumor cell models.[54]

Influence of compounds on protein synthesis

It was previously demonstrated that the alkylation of DNA suppressed the transcription and translation in cells and in *in vitro* translation systems.[49,55,56] If tumor cells were transfected with a prealkylated plasmid coding for a reporter protein GFP with *N*-methylquinolinium quinone methide, the significant suppression of GFP protein expression was detected. This inhibition was correlated with the amount of DNA adducts formed, *i.e.* the concentration of alkylating agent.[54] Moreover, if a prealkylated DNA was also used as a template for coupled transcription and translation, the significant inhibition of reporter protein expression occurs.[49,53] Therefore, to further examine whether the enhancement of tumor cells' growth inhibition is a consequence of DNA alkylation/damage by photogenerated QMs, which is produced by the irradiation of **1**, we assessed the expression of Enhanced Green Fluorescence protein (EGFP) in a cell free environment using a high-capacity T7 promoter driven *in vitro* translation system. The samples of DNA encoding the EGFP gene were incubated with compound **1** (100 μM) and psoralen and subsequently irradiated at 350 nm for 5 min or kept in dark. Afterwards, the samples were subjected to coupled transcription and translation to find a correlation between the effect of DNA damage and the amount of transcribed and subsequently translated gene product. As expected, the irradiation of psoralen almost completely inhibited the EGFP expression. Similar results were obtained previously with the cross-linking agent, cisplatin.[49] The irradiation of compound **1** led to a certain inhibition of EGFP expression, but compared to the control, irradiated DNA, this inhibition was not statistically significant, pointing to its lower alkylating potential (Fig. 8). However, in a previous study, we tested the ability of another alkylating agent, chlorambucyl, to inhibit protein translation in the same experimental system, and observed significantly lower inhibitory potency (55% of inhibition) of protein translation compared to cisplatin, or psoralen (94% of inhibition).[49] Therefore, we could observe certain inhibition, which correlates with the lower DNA alkylation ability of **1**.

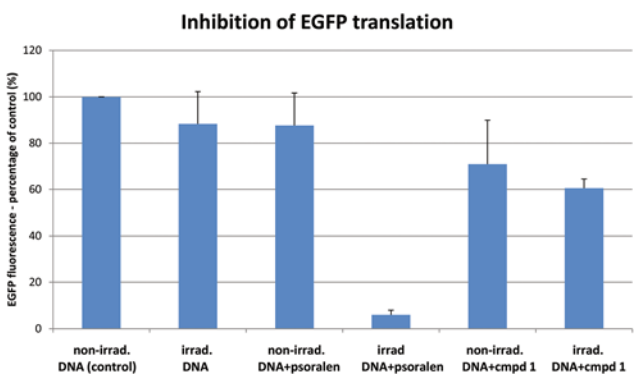

Fig. 8 Inhibition of EGFP protein translation. The plasmid containing EGFP gene under T7 promoter was incubated with psoralen (5 μM) and with compound **1** (100 μM) and was irradiated at 350 nm for 5 min (irradiated DNA), or kept in dark (non-irradiated DNA) at 24 °C. Non-irradiated DNA (positive control) and irradiated plasmid DNA without compounds were used as controls. Treated or untreated plasmid was then incubated with the S30 T7 High-Yield Protein Expression System, which enabled the EGFP protein translation/synthesis (see Experimental for details). The graph represents the percentage of EGFP fluorescence, corresponding to the amount of EGFP protein obtained during the *in vitro* translation procedure. The bars represent the average values (±SEM) of three separate experiments performed in duplicate.

Conclusions

All the investigated anthracenes moderately inhibit the proliferation of tumor cells. However, the irradiation (350 nm) of tumor cells incubated only with **1** considerably enhances the antiproliferative effect by a drastic reduction of the percentage of cells in S phase and an associated accumulation of cells in G1 and G2/M phase. This growth inhibition effect was dependent on the irradiance, whereby a longer irradiation time caused massive tumor cell death. The enhancement of the antiproliferative effect was rationalized as being due to the formation of QM **2** from **1** by excited state proton transfer, which then acts as an electrophilic species capable of reacting with biological molecules. Although the precise mechanism of the enhanced antiproliferative activity was not determined, we showed that **1** binds to DNA in a nonspecific manner causing negligible photoinduced alkylation, at variance to highlight the impediment of protein synthesis. Anthracene **1** binds also to BSA, and probably to many other proteins. Photoreaction in the presence of proteins can in principle lead to alkylation, and most likely it is the major reason for the photoinduced damage of the cellular proteins. This indication to the major role of protein-impairment is an important finding with an impact on the further development of anticancer agents based on QMs because all QM agents were sought to have DNA as the only target.

Acknowledgements

These materials are based on work financed by the Croatian Foundation for Science (HRZZ grants no. 02.05/25 and I-2364-2014), the Ministry of Science Education and Sports of the Republic of Croatia (grants no. 098-0982464-2514, 098-0982914-2918), the Natural Sciences and Engineering Research Council (NSERC) of Canada and the University of Victoria. The work was also supported by the FP7-REGPOT-2012-2013-1 project, grant agreement number 316289 – InnoMol. The authors thank Dr S. Kazazić for recording MALDI MS spectra and Dr M. Matković for the help with CD spectrometer.

Notes and references

1 *Quinone Methides*, ed. S. E. Rokita, Wiley, Hoboken, USA, 2009.

2 R. Van De Water and T. R. R. Pettus, *o*-Quinone methides: intermediates underdeveloped and underutilized in organic synthesis, *Tetrahedron*, 2002, **58**, 5367–5405.

3 T. P. Pathak and M. S. Sigman, Applications of *ortho*-Quinone Methide Intermediates in Catalysis and Asymmetric Synthesis, *J. Org. Chem.*, 2011, **76**, 9210–9215.

4 M. Freccero, Quinone Methides as Alkylating and Cross-Linking Agents, *Mini-Rev. Org. Chem.*, 2004, **1**, 403–415.

5 P. Wang, Y. Song, L. Zhang, H. He and X. Zhou, Quinone Methide derivatives: Important Intermediates to DNA Alkylating and DNA Cross-linking Actions, *Curr. Med. Chem.*, 2005, **12**, 2893–2913.

6 I. A. McDonald, P. L. Nyce, M. J. Jung and J. S. Sabol, Syntheses of DL-2-fluoromethy-p-tyrosine and DL-2-difluoromethyl-p-tyrosine as potential inhibitors of tyrosine hydroxylase, *Tetrahedron Lett.*, 1991, **32**, 887–890.

7 D. Cabaret, S. A. Adediran, M. J. G. Gonzalez, R. F. Pratt and M. Wakselman, Synthesis and Reactivity with β-Lactamases of "Penicillin-like" Cyclic Depsipeptides, *J. Org. Chem.*, 1999, **64**, 713–720.

8 S.-K. Chung, J. W. Lee, N. Y. Shim and T. W. Kwon, p-Quinone methides as geometric analogues of quinolone carboxylate antibacterials, *Bioorg. Med. Chem. Lett.*, 1996, **6**, 1309–1312.

9 Q. Wang, U. Dechert, F. Jirik and S. G. Withers, Suicide Inactivation of Human Prostatic Acid Phosphatase and a Phosphotyrosine Phosphatase, *Biochem. Biophys. Res. Commun.*, 1994, **200**, 577–583.

10 J. K. Myers, J. D. Cohen and T. S. Widlanski, Substituent Effects on the Mechanism-Based Inactivation of Prostatic Acid Phosphatase, *J. Am. Chem. Soc.*, 1995, **117**, 11049–11054.

11 J. K. Storwell, T. S. Widlanski, T. G. Kutaleladze and R. T. Raines, Mechanism-based inactivation of ribonuclease A, *J. Org. Chem.*, 1995, **60**, 6930–6936.

12 S. E. Rokita, J. Yang, P. Pande and W. A. Greenberg, Quinone Methide Alkylation of Deoxycytidine, *J. Org. Chem.*, 1997, **62**, 3010–3012.

13 W. F. Veldhuyzen, A. J. Shallop, R. A. Jones and S. E. Rokita, Thermodynamic versus Kinetic Products of DNA Alkylation as Modeled by Reaction of Deoxyadenosine, *J. Am. Chem. Soc.*, 2001, **123**, 11126–11132.

14 E. E. Weinert, K. N. Frankenfield and S. E. Rokita, Time-Dependent Evolution of Adducts Formed Between Deoxynucleosides and a Model Quinone Methide, *Chem. Res. Toxicol.*, 2005, **18**, 1364–1370.

15 E. E. Weinert, D. Ruggero, S. Colloredo-Melz, K. N. Frankenfield, C. H. Mitchell, M. Freccero and S. E. Rokita, Substituents on Quinone Methides Strongly Modulate Formation and Stability of their Nucleophilic Adducts, *J. Am. Chem. Soc.*, 2006, **128**, 11940–11947.

16 M. Chatterjee and S. E. Rokita, The Role of a Quinone Methide in the Sequence Specific Alkylation of DNA, *J. Am. Chem. Soc.*, 1994, **116**, 1690–1697.

17 Q. Zeng and S. E. Rokita, Tandem Quinone Methide Generation for Cross-Linking DNA., *J. Org. Chem.*, 1996, **61**, 9080–9081.

18 P. Pande, J. Shearer, J. Yang, W. A. Greenberg and S. E. Rokita, Alkylation of Nucleic Acids by a Model Quinone Methide, *J. Am. Chem. Soc.*, 1999, **121**, 6773–6779.

19 W. F. Veldhuyzen, P. Pande and S. E. Rokita, A Transient Product of DNA Alkylation can be Stabilized by Binding Localization, *J. Am. Chem. Soc.*, 2003, **125**, 14005–14013.

20 V. S. Li and H. Kohn, Studies on the Bonding Specificity for Mitomycin C-DNA Monoalkylation Processes, *J. Am. Chem. Soc.*, 1991, **113**, 275–283.

21 I. Han, D. J. Russell and H. Kohn, Studies on the Mechanism of Mitomycin C(1) Electrophilic Transformations: Structure-Reactivity Relationships, *J. Org. Chem.*, 1992, **57**, 1799–1807.

22 M. Tomasz, A. Das, K. S. Tang, M. G. J. Ford, A. Minnock, S. M. Musser and M. J. Waring, The Purine 2-Amino Group as the Critical Recognition Element for Sequence-Specific Alkylation and Cross-Linking of DNA by Mitomycin C, *J. Am. Chem. Soc.*, 1998, **120**, 11581–11593.

23 M. Nadai, F. Doria, M. Di Antonio, G. Sattin, L. Germani, C. Percivalle, M. Palumbo, S. N. Richter and M. Freccero, Naphthalene diimide scaffolds with dual reversible and covalent interaction properties towards G-quadruplex, *Biochemie*, 2011, **93**, 1328–1340.

24 F. Doria, M. Nadai, M. Folini, M. Di Antonio, L. Germani, C. Percivalle, C. Sissi, N. Zaffaroni, S. Alcaro, A. Artese, S. N. Richter and M. Freccero, Hybrid ligand–alkylating agents targeting telomeric G-quadruplex structures, *Org. Biomol. Chem.*, 2012, **10**, 2798–2806.

25 F. Doria, M. Nadai, M. Folini, M. Scalabrin, L. Germani, G. Sattin, M. Mella, M. Palumbo, N. Zaffaroni, D. Fabris, M. Freccero and S. N. Richter, Targeting Loop Adenines in G-Quadruplex by a Selective Oxirane, *Chem. – Eur. J.*, 2013, **19**, 78–81.

26 H. Wang, Quinone Methides and Their Biopolymer Conjugates as Reversible DNA Alkylating Agents, *Curr. Org. Chem.*, 2014, **18**, 44–60.

27 N. Basarić, K. Mlinarić-Majerski and M. Kralj, Quinone Methides: Photochemical Generation and its Application in Biomedicine, *Curr. Org. Chem.*, 2014, **18**, 3–18.

28 C. Percivalle, F. Doria and M. Freccero, Quinone Methides as DNA Alkylating Agents: An Overview on Efficient Activation Protocols for Enhanced Target Selectivity, *Curr. Org. Chem.*, 2014, **18**, 19–43.

29 L. Diao, C. Yang and P. Wan, Quinone Methide Intermediates from the Photolysis of Hydroxybenzyl Alcohols in Aqueous Solution, *J. Am. Chem. Soc.*, 1995, **117**, 5369–5370.

30 K. Nakatani, N. Higashida and I. Saito, Highly Efficient Photochemical Generation of *o*-Quinone Methide from Mannich Bases of Phenol Derivatives, *Tetrahedron Lett.*, 1997, **38**, 5005–5008.

31 E. Modica, R. Zanaletti, M. Freccero and M. Mella, Alkylation of Amino Acids and Glutathione in Water by *o*-Quinone Methide. Reactivity and Selectivity, *J. Org. Chem.*, 2001, **66**, 41–52.

32 M. Lukeman and P. Wan, Excited State Intramolecular Proton Transfer (ESIPT) in 2-Phenylphenol: An Example of Proton Transfer to a Carbon of an Aromatic Ring, *Chem. Commun.*, 2001, 1004–1005.

33 M. Lukeman and P. Wan, A New Type of Excited-State Intramolecular Proton Transfer: Proton Transfer from Phenol OH to a Carbon Atom of an Aromatic Ring Observed for 2-Phenylphenol, *J. Am. Chem. Soc.*, 2002, **124**, 9458–9464.

34 M. Lukeman and P. Wan, Excited-State Intramolecular Proton Transfer in *o*-Hydroxybiaryls: A New Route to Dihydroaromatic Compounds, *J. Am. Chem. Soc.*, 2003, **125**, 1164–1165.

35 M. Flegel, M. Lukeman and P. Wan, Photochemistry of 1,1′-Bi-2-naphthol (BINOL)-ESIPT is Responsible for Photoracemization and Photocyclization, *Can. J. Chem.*, 2008, **86**, 161–169.

36 M. Flegel, M. Lukeman, L. Huck and P. Wan, Photoaddition of Water and Alcohols to the Anthracene Moiety of 9-(2′-Hydroxyphenyl)anthracene via Formal Excited State Intramolecular Proton Transfer, *J. Am. Chem. Soc.*, 2004, **126**, 7890–7897.

37 N. Basarić and P. Wan, Competing Excited State Intramolecular Proton Transfer Pathways from Phenol to Anthracene Moieties, *J. Org. Chem.*, 2006, **71**, 2677–2686.

38 Y.-H. Wang and P. Wan, Excited State Intramolecular Proton Transfer (ESIPT) in Dihydroxyphenyl Anthracenes, *Photochem. Photobiol. Sci.*, 2011, **10**, 1934–1944.

39 P. Wang, R. Liu, X. Wu, H. Ma, X. Cao, P. Zhou, J. Zhang, X. Weng, X.-L. Zhang, J. Qi, X. Zhou and L. Weng, A potent, Water-Soluble and Photoinducible DNA Cross-Linking Agent, *J. Am. Chem. Soc.*, 2003, **125**, 1116–1117.

40 S. N. Richter, S. Maggi, S. Colloredo Mels, M. Palumbo and M. Freccero, Binol Quinone Methides as Bisalkylating and DNA Cross-Linking agents, *J. Am. Chem. Soc.*, 2004, **126**, 13973–13979.

41 F. Doria, S. N. Richter, M. Nadai, S. Colloredo-Mels, M. Mella, M. Palumbo and M. Freccero, BINOL—Amino Acid Conjugates as Triggerable Carriers of DNA-Targeted Potent Photocytotoxic Agents, *J. Med. Chem.*, 2007, **50**, 6570–6579.

42 D. Verga, S. N. Richter, M. Palumbo, R. Gandolfi and M. Freccero, Bipyridyl Ligands as Photoactivatable Mono- and Bis-Alkylating Agents Capable of DNA Cross-Linking, *Org. Biomol. Chem.*, 2007, **5**, 233–235.

43 D. Verga, M. Nadai, F. Doria, C. Percivalle, M. Di Antonio, M. Palumbo, S. N. Richter and M. Freccero, Photogeneration and Reactivity of Naphthoquinone Methides as Purine Selective DNA Alkylating Agents, *J. Am. Chem. Soc.*, 2010, **132**, 14625–14637.

44 N. Basarić, N. Cindro, D. Bobinac, K. Mlinarić-Majerski, L. Uzelac, M. Kralj and P. Wan, Sterically Congested Quinone Methides in Photodehydration Reactions of 4-Hydroxybiphenyl Derivatives and Investigation of their Antiproliferative Activity, *Photochem. Photobiol. Sci.*, 2011, **10**, 1910–1925.

45 N. Basarić, N. Cindro, D. Bobinac, L. Uzelac, K. Mlinarić-Majerski, M. Kralj and P. Wan, Zwitterionic Biphenyl Quinone Methides in Photodehydration Reactions of 3-Hydroxybiphenyl Derivatives: Laser Flash Photolysis and Antiproliferation Study, *Photochem. Photobiol. Sci.*, 2012, **11**, 381–396.

46 J. Veljković, L. Uzelac, K. Molčanov, K. Mlinarić-Majerski, M. Kralj, P. Wan and N. Basarić, Sterically Congested Adamantylnaphthalene Quinone Methides, *J. Org. Chem.*, 2012, **77**, 4596–4610.

47 S. Arumugam, J. Guo, N. E. Mbua, F. Fiscourt, N. Lin, E. Nekongo, G. J. Boons and V. V. Popik, Selective and Reversible Photochemical Derivatization of Cysteine Residues in Peptides and Proteins, *Chem. Sci.*, 2014, **5**, 1591–1598.

48 J. L. Mergny and L. Lacroix, Analysis of Thermal Melting Curves, *Oligonucleotides*, 2013, **13**, 515–537.

49 N. Perin, I. Martin Kleiner, R. Nhili, W. Laine, M.-H. David-Cordonnier, O. Vugrek, G. Karminski-Zamola, M. Kralj and M. Hranjec, Biological activity and DNA binding studies of 2-substituted benzimidazo[1,2-*a*]quinolines bearing different amino side chains, *MedChemComm*, 2013, **4**, 1537–1550.

50 M. Eriksson and B. Nordén, Linear and Circular Dichroism of Drug-Nucleic Acid Complexes, *Methods Enzymol.*, 2001, **340**, 68–98.

51 M. Nishijima, T. C. S. Pace, A. Nakamura, T. Mori, T. Wada, C. Bohne and Y. Inoue, Supramolecular Photochirogenesis with Biomolecules. Mechanistic Studies on the Enantiodifferentiation for the Photocyclodimerization of 2-Anthracenecarboxylate Mediated by Bovine Serum Albumin, *J. Org. Chem.*, 2007, **72**, 2707–2715.

52 V. Subramanian, P. Ducept, R. M. Williams and K. Luger, Effects of Photo-Chemically Activated Alkylating Agents of the FR900482 Family on Chromatin, *Chem. Biol.*, 2007, **14**, 553–563.

53 S. Bai1 and D. W. Goodrich, Different DNA Lesions Trigger Distinct Cell Death Responses in HCT116 Colon Carcinoma Cells, *Mol. Cancer Ther.*, 2004, **3**, 613–620.

54 K. Sato, Y. Kitajima, N. Kohya, A. Miyoshi, Y. Koga and K. Miyazaki, Deficient MGMT and Proficient hMLH1 Expression Renders Gallbladder Carcinoma Cells Sensitive to Alkylating Agents Through G2-M Cell Cycle Arrest, *Int. J. Oncol.*, 2005, **26**, 1653–1661.

55 A. Masta, P. J. Gray and D. R. Phillips, Nitrogen Mustard Inhibits Transcription and Translation in a Cell Free System, *Nucleic Acids Res.*, 1995, **23**, 3508–3515.

56 Q. Zhou, Y. Qu, J. B. Mangrum and X. Wang, DNA Alkylation with N-Methylquinolinium Quinone Methide to N2-dG Adducts Resulting in Extensive Stops in Primer Extension with DNA Polymerases and Subsequent Suppression of GFP Expression in A549, *Cells Chem. Res. Toxicol.*, 2011, **24**, 402–411.

